

**Distinct behavioral responses evoked by selective optogenetic stimulation of  
the major TRPV1<sup>+</sup> and MrgD<sup>+</sup> subsets of C-fibers**

Hélène Beaudry,<sup>1,2,3</sup> Ihab Daou,<sup>1,2</sup> Ariel R. Ase,<sup>1,2</sup> Alfredo Ribeiro-da-Silva,<sup>2,3</sup>  
and Philippe Séguéla<sup>1,2,\*</sup>

<sup>Φ</sup> contributed equally to this work

<sup>1</sup>Montreal Neurological Institute, Department of Neurology and Neurosurgery, <sup>2</sup>The Alan  
Edwards Centre for Research on Pain, <sup>3</sup>Department of Pharmacology and Therapeutics,  
McGill University, Montreal, Canada

# of text pages: 26

# of figures and tables: 7 figures, 0 table

**Corresponding author:**

Dr Philippe Séguéla  
Montreal Neurological Institute,  
3801 University, Suite 778  
Montreal Qc Canada H3A 2B4  
Tel: 1 (514) 398-5029  
Fax: 1 (514) 398-8106  
E-mail: philippe.seguela@mcgill.ca

## Abstract

Primary C-fiber nociceptors are broadly divided into peptidergic and non-peptidergic afferents. TRPV1 is a thermosensitive cation channel mainly localized in peptidergic nociceptors whereas MrgD is a sensory G protein-coupled receptor expressed in most non-peptidergic nociceptive afferents. TRPV1<sup>+</sup> and MrgD<sup>+</sup> fibers have been reported to be primarily involved in thermal and mechanical nociception, respectively. Yet, their functional assessment in somatosensory transmission relied on ablation strategies that do not account for compensatory mechanisms. To achieve selective activation of these two major subsets of C-fibers *in vivo* in adult mice, we used optogenetics to specifically deliver the excitatory opsin channelrhodopsin-2 (ChR2) to TRPV1<sup>+</sup> or MrgD<sup>+</sup> primary sensory neurons, as confirmed by histology and electrophysiology. This approach allowed, for the first time, the characterization of behavioral responses triggered by direct non-invasive activation of peptidergic TRPV1<sup>+</sup> or non-peptidergic MrgD<sup>+</sup> fibers in freely moving mice. Transdermal blue light stimulation of the hind paws of transgenic mice expressing ChR2 in TRPV1<sup>+</sup> neurons generated nocifensive behaviors consisting mainly of paw withdrawal and paw licking, while paw lifting occurrence was limited. Conversely, optical activation of cutaneous MrgD<sup>+</sup> afferents produced mostly withdrawal and lifting. Interestingly, in a conditioned place avoidance assay, blue light induced aversion in TRPV1-ChR2 mice, but not in MrgD-ChR2 mice. In short, we present novel somatosensory transgenic models in which control of specific subsets of peripheral unmyelinated nociceptors with distinct functions can be achieved with high spatiotemporal precision. These new tools will be instrumental in further clarifying the contribution of genetically-identified C-fiber subtypes to chronic pain.

**Keywords:** peptidergic, CGRP, P2X3, primary afferents, nociceptors, pain

## Introduction

Primary sensory neurons consist of heterogeneous cell populations that reside in sensory ganglia. Their terminals in peripheral tissues transduce noxious and innocuous stimuli of different modalities - mechanical, thermal and/or chemical. The diversity of these neurons has been defined at the functional, electrophysiological and molecular levels. Their neurochemical characterization revealed a number of genetic markers used to classify them and/or associate them with specific functions.

Heat transduction in C-fiber nociceptors has been mainly attributed to the TRPV1 channel but its deletion in mice had partial effects on noxious heat sensitivity, indicating the presence of other noxious heat sensors [3; 4; 8]. Interestingly, ablation of TRPV1<sup>+</sup> fibers produced a complete loss of thermal sensitivity in mice, arguing that this neuronal population is necessary for the detection of thermal stimuli [6]. In mice, TRPV1 is a marker of the peptidergic subset of sensory neurons characterized by the expression of neuroactive and vasoactive peptides such as CGRP and SP. Anatomically, peptidergic afferents project to lamina I and the outer part of lamina II of the dorsal horn of the spinal cord [1; 13; 20]. On the other hand, most non-peptidergic nociceptors express the purinergic receptor P2X3 and bind the isolectin IB4. The Mas-related G protein-coupled receptor subtype D (MrgD) has been identified as a marker of this subpopulation as its expression covers most P2X3<sup>+</sup> neurons. Non-peptidergic primary afferents project centrally to the middle/inner part of lamina II of the dorsal horn and terminate peripherally as free nerve endings mostly in the skin epidermis and dermis [13; 20; 21; 25]. Ablation of MrgD<sup>+</sup> neurons significantly reduced mechanical sensitivity with mice displaying higher von Frey thresholds under normal and inflammatory conditions [6].

Selective modulation of these neuronal subsets is valuable in dissecting their differential contribution to nociception and chronic pain. Although useful, ablation strategies have the caveat of potential compensatory mechanisms in somatosensory circuits. Here, we describe optogenetic approaches to achieve precise and selective activation of two major genetically-identified and non-overlapping subpopulations of adult nociceptors.

Optogenetics consists of the heterologous expression of photosensitive actuators, such as channelrhodopsin-2 (ChR2), to modulate cellular activity with high spatiotemporal resolution [18; 19]. By targeting ChR2-Venus to the MrgD locus, Wang and Zylka selectively activated MrgD<sup>+</sup> fibers and assessed their connectivity to second-order neurons in the dorsal horn of spinal cord. However, they did not report any behavioral results, presumably due to low opsin levels insufficient to drive light-induced responses [24]. To overcome this limitation and avoid any non-specific opsin expression due to developmental regulation of MrgD [15], we used an inducible, Cre-dependent strategy to deliver ChR2 to mature MrgD<sup>+</sup> nociceptors. On the other hand, knowing that TRPV1 expression is also developmentally modulated [5] and due to the lack of an inducible TRPV1-Cre transgenic line, we used the constitutive TRPV1-Cre mouse line coupled to a viral delivery approach to induce the selective expression of ChR2 in TRPV1<sup>+</sup> dorsal root ganglia (DRG) neurons in adult mice. We report here the functional phenotyping of the *TRPV1-ChR2* and *MrgD-ChR2* mouse lines based on histological, electrophysiological and behavioral analysis.

## Materials and Methods

### Transgenic mouse lines

Six- to sixteen-week-old *TRPV1-ChR2* or *MrgD-ChR2* mice of both sexes, weighing 20–35 g, were used in this study. Animals were kept on a 12:12-hour light/dark cycle, with food and water provided *ad libitum*. All animal procedures were performed in accordance with the McGill University Animal Care Committee regulations.

Homozygous *TRPV1-Cre* mice (The Jackson Laboratory) were injected intrathecally with an AAV2/8 virus [AAV2/8-CAG-*floxed stop-ChR2(H134R)-tdTomato-WPRE*] at the age of 6 weeks to generate *TRPV1-ChR2* mice. This approach allowed us to deliver the opsins after the developmental regulation of TRPV1 has occurred [5]. Intrathecal injections were done free hand in non-anesthetized mice as described previously [10; 11]. Briefly, a 30 g ½-in. needle connected to a length of PE10 tubing and attached to a 50 µl Luer-hub Hamilton syringe was inserted into the L5–L6 intervertebral space (at the level of the cauda equina) and virus (5 µl; titer > 5 X 10<sup>12</sup> gc/ml) was injected over a 2 s time period. Appropriate placement of the needle was confirmed by observing a brief twitch of the tail. Experiments were conducted 4 to 6 weeks post-injection since ChR2 expression decreased after this time (confirmed by decreased light-induced pain behaviors).

Homozygous *MrgD<sup>CreERT2</sup>* mice (kindly provided by Dr. Wenqin Luo, University of Pennsylvania) were crossed with homozygous Ai32 mice (The Jackson Laboratory). *MrgD<sup>CreERT2</sup>* mice carry the *CreERT2* construct separated by an *IRES* cassette from the last *MrgD* coding exons, allowing its expression under the control of the *MrgD* promoter without interference with normal *MrgD* transcription. Ai32 mice carry in the *ROSA26* locus the *floxed stop-ChR2(H134R)-EYFP* construct [17]. These crossings generated the *MrgD-ChR2* transgenic mouse line. All experimental animals were heterozygous for both *MrgD* and the *ROSA26* transgene. To induce

opsin expression in *MrgD-ChR2* mice, tamoxifen (100  $\mu$ L, 10 mg/mL) was injected intraperitoneally for 5 consecutive days starting at P14, alternating between the sides of injection. To control for tamoxifen injections, the same procedure was performed on heterozygous *MrgD<sup>CreERT2</sup>* mice.

### **Immunofluorescence**

Mice were intracardially perfused with 50 mL saline, followed by 50 mL of ice-cold 4% paraformaldehyde (PFA) in 0.1 M phosphate buffer, pH 7.4. DRG, spinal cord, and glabrous skin were extracted and post-fixed in 4% PFA for 1 h at room temperature. Tissue was then cryoprotected in 30% sucrose in 0.01 M phosphate buffered saline (PBS) overnight at 4 °C. To study the spinal cord, 30  $\mu$ m-thick sections were cut at -20 °C using a cryostat (Leica) collected as free-floating in PBS containing 0.2 % Triton-X (PBS-T). As for the DRG and skin, sectioning at 14  $\mu$ m thickness was performed directly onto gelatin-subbed slides. Sections were washed in PBS-T for 30 min between all incubations. Nonspecific binding of the secondary antibody was blocked by pre-treating the sections for 1 h at room temperature in 10% normal goat serum and 10% normal donkey serum (Invitrogen) diluted in PBS-T. The sections were then incubated at 4 °C for 24 h with a rabbit anti-CGRP antibody (Sigma-Aldrich #C8198, 1:2000) or a guinea pig anti-P2X3 antibody (Neuromics #GP10108, 1:25000). After several rinses in PBS-T, sections were incubated for 90 min at room temperature with a biotin-conjugated donkey anti-guinea pig IgG (1:200; Jackson ImmunoResearch) in PBS, followed by additional signal amplification via tyramide (1:75; PerkinElmer Life and Analytical Sciences) for 7 min. After several rinses in PBS-T, the sections were incubated for 2 h at room temperature with streptavidin conjugated to Alexa Fluor 488 (1:200; Invitrogen), Isolectin IB4 conjugated to Alexa Fluor 568 or highly cross-absorbed goat anti-rabbit IgG conjugated to Alexa Fluor 568 (1:1000; Invitrogen) in PBS-

T. Finally, the sections were washed, mounted on gelatin-subbed slides (spinal cord), air-dried and cover slipped with anti-fading mounting medium (Aqua PolyMount, Polysciences). Slides were stored at 4 °C until examination under a Zeiss LSM 710 confocal microscope. The percentage of tdTomato<sup>+</sup> cells expressing P2X3 or CGRP and the percentage of EYFP<sup>+</sup> cells expressing CGRP or binding IB4 were quantified in DRG sections from *TRPV1-ChR2* and *MrgD-ChR2* mice respectively.

### **Cell culture and DRG preparation**

DRGs were extracted from adult *TRPV1-ChR2* or *MrgD-ChR2* mice and kept in sterile ice-cold 1x HBSS Hanks medium (Invitrogen) throughout the dissection. DRGs were then incubated in 5 mL of HBSS containing 1.4 mg/mL dispase (Sigma-Aldrich) and 1.1 mg/mL collagenase type II (Sigma-Aldrich) for 45 min at 37 °C. Following the enzymatic reaction, DRGs were washed once with F-12 culture media (Invitrogen), containing 10% FBS, 1% L-Glutamine, 1% penicillin, and 1% streptomycin, and then mechanically triturated using fire-polished Pasteur pipettes. The dissociated neurons were finally plated onto 35 mm culture dishes (Sarstedt, 2 mL/dish) previously coated with laminin (BD Bioscience) and poly-D-lysine (Sigma-Aldrich). Cells were incubated for 2 h at 37 °C and 5% CO<sub>2</sub> prior to electrophysiological recording. Since a significant downregulation of capsaicin responses was observed in *TRPV1-ChR2* neurons 24 to 72 h after plating (data not shown), electrophysiological recordings were conducted using freshly dissociated DRG neurons.

## **Electrophysiology**

Whole-cell patch-clamp recordings on DRG neurons were conducted at room temperature, 2 to 6 h after plating. The pipette's internal solution (pH 7.2) contained the following in mM: 130 K-gluconate, 1 MgCl<sub>2</sub>, 10 HEPES, 5 EGTA, 3 MgATP, and 0.4 GTP. The bath solution, pH 7.4, contained the following in mM: 152 NaCl, 5 KCl, 2 CaCl<sub>2</sub>, 1 MgCl<sub>2</sub>, 10 HEPES, and 10 glucose. Patch pipettes had a tip resistance of 5–10 MΩ. Electrophysiological recordings were conducted using an Axopatch 200B amplifier, digitized with a Digidata 1322A interface (Axon Instruments). Traces were acquired and analyzed using pClamp 8.2 software (Axon Instruments). Recordings were low-pass filtered at 2 KHz and 5 KHz in voltage and current clamp configurations, respectively. Multimode optic fibers (200 μm diameter; Thorlabs), coupled to diode-pumped solid-state lasers of specific wavelengths (473 nm blue laser, Laserglow Technologies; or 589 nm yellow laser, Dragon Lasers), were used for optical stimulation of DRG neurons. Stimulation parameters are specified in each condition. Light intensities were measured using a PM100A power meter coupled to a S130C photodiode sensor (Thorlabs) and analyzed using LabVIEW 8.5.

## **Acute light-induced nocifensive behaviors**

Mice were habituated for 1 h in transparent Plexiglas cubicles set atop a ½-inch glass floor and separated from each other by opaque dividers. Acute nocifensive behaviors were elicited using a pulsing laser (473 nm blue light, at 2, 5, and 10 Hz) set at different intensities and aimed at the plantar surface of the hind paws. For each condition, three 20 s trials were conducted, alternating between the left and right hind paws with at least 3 min between trials. Scored nocifensive behaviors included purposeful hind paw withdrawal, hind paw licking and hind paw lifting. Hind paw withdrawal consisted of paw removal to avoid the optical stimulus followed immediately by

replacing the paw on the glass floor. Hind paw lifting consisted of removing the paw and keeping it lifted for a prolonged period of time. The percentage of trials in which these behaviors occurred is reported. The number of paw withdrawals and the time spent lifting or licking per trial were also quantified in the trials where such behaviors occurred. In control animals not expressing ChR2, optical stimulation (2, 5, and 10 Hz) did not produce any behavior, even when the highest light intensity was applied for 20 seconds (see Supplementary Materials for video).

### **Light-induced conditioned place aversion assay**

A shuttle box, composed of two equal-sized compartments with distinct visual cues (one has horizontal black stripes and the other has vertical black stripes) placed over a glass surface was used for a consecutive 5-day experimental procedure. On day 1, during habituation sessions 1 and 2, mice freely explored the two compartments for 10 min. On sessions 3 to 8, in the control condition, each mouse received yellow light illumination (2 Hz, 8 mW/mm<sup>2</sup> for 10 min) on the right hind paw, and was confined to the non-pain-paired compartment during illumination; in the experimental condition, the left hind paw was stimulated with blue light (2 Hz, 8 mW/mm<sup>2</sup> for 10 min), and was confined to the pain-paired compartment. On day 5 (test session), each mouse was allowed to freely explore the two compartments for 5 min, and the time spent in each compartment was recorded. The percent time spent in each compartment was calculated by dividing the time spent in that particular compartment by the time spent in both compartments multiplied by 100. Conditioning sessions were balanced so half the mice had the horizontal black stripe compartment as the pain-paired compartment while the other half had the vertical black stripe compartment associated with the painful stimulus. Sessions were also balanced so half of the mice received blue light first while the other half received yellow light first.

## Data analysis

Data analysis was performed in Excel, graphs plotted in SigmaPlot 11, and statistics (Student's t-test or two-way ANOVA) analyzed in Prism GraphPad 6. Data are expressed as the mean  $\pm$  SEM, P-values are indicated in the figure legends.

## Results

### Cellular distribution of ChR2 in TRPV1<sup>+</sup> or MrgD<sup>+</sup> neurons

To investigate the expression profile of ChR2 opsins in the peripheral pathways of *TRPV1-ChR2* mice, we visualized the endogenous ChR2-tdTomato fluorescence directly and immunostained for the non-peptidergic marker P2X3, normally absent in TRPV1<sup>+</sup> afferents. In the dorsal horn of the spinal cord, bright tdTomato fluorescence was detected exclusively in lamina I and outer lamina II, dorsal to the green signal of non-peptidergic P2X3<sup>+</sup> fibers, in a region well known to be innervated by peptidergic primary afferents (Fig. 1A) [5]. In the periphery, tdTomato<sup>+</sup> free nerve endings were rather sparse and did not overlap with P2X3<sup>+</sup> fibers (Fig 1B). The small number of tdTomato<sup>+</sup> fibers seen in the skin most probably reflects the relatively low number of DRG neurons transduced by the intrathecal delivery of ChR2-tdTomato (Fig 1C). Indeed, only  $15.6 \pm 1.6\%$  of CGRP<sup>+</sup> DRG neurons expressed tdTomato. All (100%) TdTomato<sup>+</sup> cells were small diameter sensory neurons expressing CGRP, while a small proportion of them were found to be positive for P2X3 ( $4.1 \pm 2.0\%$ , 4 out of 88 neurons) (Fig 1C). Our data confirm the selective expression of ChR2-tdTomato in TRPV1<sup>+</sup>/CGRP<sup>+</sup> nociceptive neurons and its efficient trafficking to the most distal ends of the primary afferents.

Conversely, to assess the exclusive expression of ChR2 channels in non-peptidergic sensory neurons of *MrgD-ChR2* mice, we performed immunostaining for the peptidergic marker CGRP,

expecting virtually no overlap with the cellular distribution of ChR2-EYFP. Direct EYFP fluorescence signal was strong in DRG, spinal cord and glabrous skin, indicating that tamoxifen administration efficiently induced ChR2-EYFP expression and that opsins are well trafficked to both central and peripheral terminals. In the dorsal horn of the spinal cord, the EYFP signal was detected in the inner part of lamina II (lamina II<sub>i</sub>), ventral to the area of termination of CGRP afferents, demonstrating the selective expression of ChR2-EYFP in non-peptidergic nociceptive neurons (Fig. 2A). In the periphery, EYFP<sup>+</sup> fibers terminated as free nerve endings often extending more superficially in the epidermis than CGRP<sup>+</sup> fibers (Fig. 2B). All (100%) EYFP<sup>+</sup> DRG neurons were positive for the non-peptidergic marker IB4 while  $76.4 \pm 4.3\%$  of IB4<sup>+</sup> neurons were EYFP<sup>+</sup>, demonstrating that this inducible transgenic approach achieved a high coverage of the non-peptidergic C-fiber subset. Only  $0.92 \pm 0.68\%$  (3 out of 310) of EYFP<sup>+</sup> neurons expressed CGRP (Fig 2C). Collectively, the absence of overlap between the EYFP and CGRP signals, the central projection of EYFP<sup>+</sup> fibers to lamina II<sub>i</sub> of the dorsal horn, and the superficial innervation of the epidermis by EYFP<sup>+</sup> free nerve endings are consistent with the chemo-anatomical profile of MrgD<sup>+</sup> fibers [25] and validate the exclusive expression of ChR2-EYFP channels in MrgD<sup>+</sup> non-peptidergic afferents.

### **Functionality of the opsins in TRPV1<sup>+</sup> or MrgD<sup>+</sup> DRG neurons**

To test the functionality of the optogenetic constructs, we conducted patch clamp electrophysiology on acutely dissociated DRG neurons from adult *TRPV1-ChR2* and *MrgD-ChR2* mice. Blue light stimulation induced significant inward photocurrents in neurons from both *TRPV1-ChR2* and *MrgD-ChR2* mice, (peak current density of  $27.83 \pm 3.27$  and  $14.08 \pm 1.67$  pA/pF for *TRPV1-ChR2* and *MrgD-ChR2* respectively) exhibiting typical ChR2 current phenotype and kinetics. Furthermore, short blue light pulses delivered at 1 Hz frequency were

sufficient to reliably evoke action potentials in either tdTomato<sup>+</sup> or EYFP<sup>+</sup> neurons (Fig. 3A,B), suggesting that transdermal optical stimulation may efficiently activate these specific subsets of primary afferents *in vivo*. Crucially, every photosensitive *TRPV1-ChR2* DRG neuron displayed an inward TRPV1-mediated current evoked by capsaicin application [4] (100%, 11/11 neurons; Fig. 3A,C). Similarly, all blue light-sensitive DRG neurons from *MrgD-ChR2* mice responded to the selective P2X3 agonist  $\alpha,\beta$ -meATP with typical homomeric P2X3 currents [9] (100%, 8/8 neurons; Fig. 3B,C). Unexpectedly, our recordings showed that within the TRPV1<sup>+</sup> population responding to both blue light and capsaicin, some cells also responded to  $\alpha,\beta$ -meATP (6/11 neurons) (Fig. 3B,C). Conversely, 3 out of 8 MrgD<sup>+</sup> neurons responded to capsaicin in addition to  $\alpha,\beta$ -meATP and blue light (Fig 3C). However different P2X current profiles were recorded in the two subsets of nociceptors: *MrgD-ChR2* DRG neurons consistently displayed homomeric P2X3 channels while *TRPV1-ChR2* neurons mainly expressed heteromeric P2X2+3 channels (Fig. 3C). Nevertheless, our patch clamp data confirm that all ChR2<sup>+</sup> neurons from *TRPV1-ChR2* mice express TRPV1 while all ChR2<sup>+</sup> neurons from *MrgD-ChR2* mice express P2X3.

### **Acute light-induced behavioral responses in *TRPV1-ChR2* and *MrgD-ChR2* mice**

To assess whether selective activation of TRPV1<sup>+</sup> or MrgD<sup>+</sup> fibers induces behavioral responses in freely moving mice, we transdermally stimulated the glabrous skin of the hind paws of *TRPV1-ChR2* or *MrgD-ChR2* mice with blue light (473 nm) using a range of increasing intensities (2.19–7.93 mW/mm<sup>2</sup>) and increasing pulsing frequencies (2, 5, and 10 Hz). In *TRPV1-ChR2* mice, the main behaviors detected under optical stimulation were paw withdrawal (Fig. 4A,B), paw lifting (Fig.4C) and paw licking (Fig. 4D), whereas paw lifting occurred less frequently even at high laser intensities (Fig. 4C). Although not significant, the light-induced nocifensive behaviors tended to be intensity-dependent, except for light-evoked lifting (Fig. 4C).

In *MrgD-ChR2* mice, the predominant behaviors under optical illumination consisted of paw withdrawal (Fig. 5A and 5B) and paw lifting (Fig. 5C). Paw licking also occurred, although to a lesser extent (Fig. 5D). The profile of these nocifensive behaviors was not significantly different across the various optical parameters tested, indicating that nocifensive responses were saturated at the lowest light intensity and that these behaviors are frequency-independent. The behavioral profile of *MrgD-ChR2* mice in response to blue light was globally milder than that of *Nav1.8-ChR2*<sup>+</sup> mice that exhibited robust paw withdrawal, paw licking, jumping and audible vocalization in response to similar stimulation parameters [7]. Altogether, our data confirm the expression of ChR2 in the glabrous skin of both *TRPV1-ChR2* and *MrgD-ChR2* mice and indicate that the level of expression is sufficiently high to generate nocifensive behaviors in freely moving mice. Our data also show that peripheral activation of peptidergic TRPV1<sup>+</sup> or non-peptidergic MrgD<sup>+</sup> C-fiber primary afferents in the glabrous skin drives distinct behavioral responses.

The most striking difference in light-induced behaviors between *TRPV1-ChR2* and *MrgD-ChR2* mice was the total time they spent licking or lifting the illuminated paw, respectively (see Supplementary Materials for video recordings of representative light-induced behavioral responses in these two ChR2-expressing mouse lines and in a control mouse line). Indeed, *TRPV1-ChR2* mice spent significantly more time licking the stimulated paw than *MrgD-ChR2* mice at 2, 5 and 10 Hz pulsing frequencies (Fig. 6A). Conversely, *MrgD-ChR2* mice never licked for a prolonged time when blue light was applied to the hind paw. This was also the case at maximum light intensity. Interestingly, the time spent licking the paw in *TRPV1-ChR2* mice was intensity-dependent (Fig. 6A). On the other hand, *MrgD-ChR2* mice spent significantly more time lifting their paws at 2, 5 and 10 Hz than *TRPV1-ChR2* mice (Fig. 6B). Quantitative analysis

of the light-evoked responses of *TRPV1-ChR2* and *MrgD-ChR2* mice led us to propose that these behaviors reflect qualitatively different somatosensory perceptions.

### **Light-induced aversion in *TRPV1-ChR2*, not in *MrgD-ChR2* mice**

In order to investigate the association of acute light-induced behaviors with the activation of supraspinal regions, we used the conditioned place aversion paradigm to assess the aversive motivational effects of activating *TRPV1*<sup>+</sup> or *MrgD*<sup>+</sup> primary afferents (Fig. 7A). In absence of optical stimulation or under yellow light stimulation (negative control), mice showed no preference to a particular compartment (Fig. 7B,C). However, blue light was clearly aversive to *TRPV1-ChR2* mice. Indeed, *TRPV1-ChR2* mice spent significantly less time in the blue light-paired (painful) compartment compared to the yellow light-paired compartment (Fig. 7D). Interestingly, no place avoidance was observed in *MrgD-ChR2* mice using the same conditioning parameters (Fig. 7D), revealing different degrees of aversion between *TRPV1*<sup>+</sup> and *MrgD*<sup>+</sup> C-fiber activation, with potentially a non-aversive/non-painful somatosensory perception following *MrgD*<sup>+</sup> fiber activation. Altogether, these results indicate a differential central processing of specific peripheral nociceptive inputs driving distinctive associative and motivational behaviors in mice.

## Discussion

In this study, we present novel optogenetic mouse lines to specifically investigate functional differences in two major subsets of C fiber nociceptors. Altogether, our results demonstrate the potential of these novel tools to investigate the physiological role of peptidergic and non-peptidergic subpopulations of small diameter nociceptors *in vivo*. Taking advantage of the *TRPV1-Cre* and *MrgD<sup>CreERT2</sup>* driver lines, we selectively delivered optogenetic actuators to TRPV1<sup>+</sup> peptidergic and MrgD<sup>+</sup> non-peptidergic neurons that together form the majority of nociceptors with minimal overlap [6]. In *MrgD-ChR2* mice, the Cre-dependent expression of excitatory ChR2 channels was driven by the CAG promoter, overcoming the limitation of low opsin levels [24]. Moreover, the inducible *Cre<sup>ERT2</sup>* construct allowed us to circumvent developmental regulation of the MrgD gene [15]. To restrict opsin expression to the adult DRG population in *TRPV1-ChR2* mice [5], we intrathecally infected *TRPV1-Cre* adult mice with Cre-dependent AAVs. These approaches allowed for the first time the induction of light-induced pain behaviors by selectively activating peptidergic or non-peptidergic subsets of primary afferents in freely moving mice.

Histological analysis validated the selective expression of ChR2 in MrgD<sup>+</sup> or TRPV1<sup>+</sup> neurons. In *TRPV1-ChR2* mice, 100% of ChR2<sup>+</sup> cells were positive for the peptidergic marker CGRP and their central terminals were found mostly in lamina I and outer lamina II of the spinal cord, as expected [5]. Conversely, in *MrgD-ChR2* mice, the almost exclusive expression of ChR2 in small diameter DRG neurons, its dorsal horn termination area restricted to lamina Iii, as well as its termination as free nerve endings in the superficial part of the skin, are all consistent with the previously described anatomical distribution of MrgD<sup>+</sup> afferents [25]. Moreover, the fact that

100% of ChR2<sup>+</sup> DRG neurons of *MrgD-ChR2* mice expressed the marker IB4 confirms the selective targeting of non-peptidergic C fibers. Our histological data confirm that both our transgenic strategies are effective to overcome developmental gene regulation that could lead to nonspecific expression in adult nociceptors [6; 16].

Our electrophysiological analysis showed that transgenic ChR2 opsins were efficient at driving firing activity, as photocurrents reliably induced action potentials in cultured DRG neurons from either *MrgD-ChR2* or *TRPV1-ChR2* mice. Moreover, 100% of ChR2<sup>+</sup> neurons from *MrgD-ChR2* mice responded to  $\alpha,\beta$ -meATP and 100% of ChR2<sup>+</sup> from *TRPV1-ChR2* mice responded to capsaicin, demonstrating that there is no leakage in the transgenic expression of ChR2 and that its expression is faithful to the targeted cell population. These results were correlated with our histological analysis showing that around 4% of TRPV1<sup>+</sup> neurons were positive for the non-peptidergic marker P2X3 and around 1% of MrgD<sup>+</sup> neurons were positive for the peptidergic marker CGRP. Interestingly, in patch clamp recordings we observed that 55% of TRPV1<sup>+</sup> neurons responded to  $\alpha,\beta$ -meATP while 38% of MrgD<sup>+</sup> neurons were capsaicin-sensitive, although with significantly smaller current densities than with their cognate agonist. A possible explanation for the discrepancy between our histological and electrophysiological data is that the process of isolation and dissociation of DRG neurons changes their gene expression, leading to a different profile than *in vivo*. Although a RNA sequencing study showed some overlap between mouse peptidergic and non-peptidergic populations with a small fraction of neurons co-expressing TRPV1 and P2X3 mRNA [22], our data confirm that ChR2 expression is restricted to two mutually exclusive populations of C-fiber nociceptors *in vivo*.

Based on the previous characterization of behavioral responses to acute transdermal illumination in *Nav1.8-ChR2*<sup>+</sup> mice [7], we evaluated the nocifensive behaviors generated by blue light stimulation of the plantar surface of the hind paws of *TRPV1-ChR2* and *MrgD-ChR2* mice. Acute illumination of the hind paw of *TRPV1-ChR2* mice mainly generated prolonged licking behaviors whereas activation of cutaneous *MrgD*<sup>+</sup> fibers mainly produced prolonged hind paw lifting responses. In both lines, these responses were milder than those observed previously in *Nav1.8-ChR2*<sup>+</sup> mice [7]. Since the *Nav1.8*<sup>+</sup> population is larger than the *TRPV1*<sup>+</sup> or *MrgD*<sup>+</sup> nociceptive populations, these results suggest that the intensity of the behavioral responses depends on the number of sensory afferents recruited by the optical stimulation. Furthermore, licking in *MrgD-ChR2* mice was limited compared to *TRPV1-ChR2* mice that display fast and prolonged paw licking in response to acute blue light, in agreement with the role of *TRPV1*<sup>+</sup> in thermoreception and burning sensation. This difference in evoked stereotypical responses suggests that a behavioral output can be solely dictated by the subset of peripheral primary afferents activated. This provides evidence that basic sensory modalities can be coded early on in the pain pathways (labeled line) before they are differentially processed in the spinal cord and higher in the brain.

In addition to the phenotyping of acute behaviors upon light stimulation, we assessed the role of *TRPV1*<sup>+</sup> and *MrgD*<sup>+</sup> fibers in more complex spontaneous behaviors. Using the conditioned place aversion paradigm, we showed that transdermal blue light stimulation of the paw in *TRPV1-ChR2* mice represents a strong avoidance cue. Interestingly, despite the acute behaviors observed under light stimulation in *MrgD-ChR2* mice, no clear preference or avoidance was detected under these conditioning settings. One possible reason for this significant difference is that acute behaviors generated under optical stimulation are weaker in *MrgD-ChR2* compared to *TRPV1-*

*ChR2* mice. One could argue that it is a matter of transgene penetrance, but our histological data show that the opsin is strongly expressed in most MrgD<sup>+</sup> C-fiber afferents in *MrgD-ChR2* mice. Moreover, the maximal optical activation of MrgD<sup>+</sup> fibers was reached since acute behaviors did not change with increasing light intensity. In mice, peptidergic fibers are known to be involved in thermosensation whereas non-peptidergic fibers transmit mechanical nociception [6]. As distinct acute optically-induced behaviors were obvious between the two mouse lines, another possibility is that activation of MrgD<sup>+</sup> fibers, presumably mechanosensitive, triggers an aching, dull pain that is not sufficiently aversive to generate a place conditioning compared to activation of TRPV1<sup>+</sup> fibers that triggers a sharp, burning pain. Alternatively, the interpretation of the behaviors detected in *MrgD-ChR2* mice as nocifensive may not be accurate. Mice may withdraw or lift their paws due to unpleasantness which may not be sufficient to drive aversion. Another explanation for the absence of avoidance behavior in *MrgD-ChR2* mice may be that optical activation of a neuronal subset in isolation has not the same physiological impact as the synergistic activation of several types of mechanosensitive fibers evoked by natural stimuli. Our findings suggest that activation of the circuitry involving solely TRPV1<sup>+</sup> fibers has a more direct aversive effect. A study suggested a predominant role of non-peptidergic nociceptors in the affective component of pain [2], but this anatomical study was not corroborated with behavioral data. Genetically, the MrgD<sup>+</sup> afferents and the MrgB4<sup>+</sup> afferents, involved in the pleasant perception of stroking [23], belong to the same Ret-dependent lineage of unmyelinated cutaneous non-peptidergic C-fibers [12; 14; 22]. It is therefore possible also that activation of MrgD<sup>+</sup> neurons is perceived as weakly aversive or even pleasant when appropriately tuned.

Altogether, we present new transgenic models in which specific subsets of C-fiber nociceptors are optogenetically controlled, leading to distinct nocifensive behaviors that translate into

different aversion profiles in adult mice. This approach allowed for the first time the selective and temporally-precise activation of TRPV1<sup>+</sup> or MrgD<sup>+</sup> fibers in non-anesthetized, freely moving mice and the characterization of the behavioral profile generated. This work not only provides new tools to tackle the physiological complexity of peripheral somatosensory pathways but also opens the door to the understanding of the contribution of various neuronal subsets to pain perception under chronic conditions.

### **Acknowledgements**

We thank Noosha Youssefpour, Van Nguyen and Manon St-Louis for their technical support and Dr. Anna Taylor (Hatos Center for Neuropharmacology, UCLA) for her help in video processing. H. Beaudry was supported by a postdoctoral fellowship from the Fonds de Recherche du Québec- Santé and the Canadian Arthritis Society. I. Daou received a scholarship from Fonds de Recherche du Québec- Santé. A. Ribeiro-Da-Silva was supported by the Canadian Institutes of Health Research, the Quebec Pain Research Network and the Louise and Alan Edwards Foundation. P. Séguéla was supported by the Canadian Institutes of Health Research, the Natural Sciences and Engineering Research Council, the Quebec Pain Research Network and the Louise and Alan Edwards Foundation.

### **Conflict of Interest Statement**

The authors have nothing to declare.

## References

- [1] Basbaum AI, Bautista DM, Scherrer G, Julius D. Cellular and Molecular Mechanisms of Pain. *Cell* 2009;139(2):267-284.
- [2] Braz JM, Nassar MA, Wood JN, Basbaum AI. Parallel "pain" pathways arise from subpopulations of primary afferent nociceptor. *Neuron* 2005;47(6):787-793.
- [3] Caterina MJ, Leffler A, Malmberg AB, Martin WJ, Trafton J, Petersen-Zeitl KR, Koltzenburg M, Basbaum AI, Julius D. Impaired nociception and pain sensation in mice lacking the capsaicin receptor. *Science* 2000;288(5464):306-313.
- [4] Caterina MJ, Schumacher MA, Tominaga M, Rosen TA, Levine JD, Julius D. The capsaicin receptor: a heat-activated ion channel in the pain pathway. *Nature* 1997;389(6653):816-824.
- [5] Cavanaugh DJ, Chesler AT, Braz JM, Shah NM, Julius D, Basbaum AI. Restriction of transient receptor potential vanilloid-1 to the peptidergic subset of primary afferent neurons follows its developmental downregulation in nonpeptidergic neurons. *The Journal of neuroscience : the official journal of the Society for Neuroscience* 2011;31(28):10119-10127.
- [6] Cavanaugh DJ, Lee H, Lo L, Shields SD, Zylka MJ, Basbaum AI, Anderson DJ. Distinct subsets of unmyelinated primary sensory fibers mediate behavioral responses to noxious thermal and mechanical stimuli. *Proceedings of the National Academy of Sciences of the United States of America* 2009;106(22):9075-9080.
- [7] Daou I, Tuttle AH, Longo G, Wieskopf JS, Bonin RP, Ase AR, Wood JN, De Koninck Y, Ribeiro-da-Silva A, Mogil JS, Seguela P. Remote optogenetic activation and sensitization of pain pathways in freely moving mice. *J Neurosci* 2013;33(47):18631-18640.
- [8] Davis JB, Gray J, Gunthorpe MJ, Hatcher JP, Davey PT, Overend P, Harries MH, Latcham J, Clapham C, Atkinson K, Hughes SA, Rance K, Grau E, Harper AJ, Pugh PL, Rogers DC, Bingham S, Randall A, Sheardown SA. Vanilloid receptor-1 is essential for inflammatory thermal hyperalgesia. *Nature* 2000;405(6783):183-187.
- [9] Dussor G, Zylka MJ, Anderson DJ, McCleskey EW. Cutaneous sensory neurons expressing the Mrgprd receptor sense extracellular ATP and are putative nociceptors. *Journal of neurophysiology* 2008;99(4):1581-1589.
- [10] Fairbanks CA. Spinal delivery of analgesics in experimental models of pain and analgesia. *Adv Drug Deliv Rev* 2003;55(8):1007-1041.
- [11] Hylden JL, Thomas DA, Iadarola MJ, Nahin RL, Dubner R. Spinal opioid analgesic effects are enhanced in a model of unilateral inflammation/hyperalgesia: possible involvement of noradrenergic mechanisms. *Eur J Pharmacol* 1991;194(2-3):135-143.
- [12] Lallemand F, Ernfors P. Molecular interactions underlying the specification of sensory neurons. *Trends Neurosci* 2012;35(6):373-381.
- [13] Le Pichon CE, Chesler AT. The functional and anatomical dissection of somatosensory subpopulations using mouse genetics. *Frontiers in neuroanatomy* 2014;8:21.
- [14] Li CL, Li KC, Wu D, Chen Y, Luo H, Zhao JR, Wang SS, Sun MM, Lu YJ, Zhong YQ, Hu XY, Hou R, Zhou BB, Bao L, Xiao HS, Zhang X. Somatosensory neuron types identified by high-coverage single-cell RNA-sequencing and functional heterogeneity. *Cell Res* 2016;26(8):967.
- [15] Liu Y, Yang FC, Okuda T, Dong X, Zylka MJ, Chen CL, Anderson DJ, Kuner R, Ma Q. Mechanisms of compartmentalized expression of Mrg class G-protein-coupled sensory

- receptors. *The Journal of neuroscience : the official journal of the Society for Neuroscience* 2008;28(1):125-132.
- [16] Luo W, Enomoto H, Rice FL, Milbrandt J, Ginty DD. Molecular identification of rapidly adapting mechanoreceptors and their developmental dependence on ret signaling. *Neuron* 2009;64(6):841-856.
- [17] Madisen L, Mao T, Koch H, Zhuo JM, Berenyi A, Fujisawa S, Hsu YW, Garcia AJ, 3rd, Gu X, Zanella S, Kidney J, Gu H, Mao Y, Hooks BM, Boyden ES, Buzsaki G, Ramirez JM, Jones AR, Svoboda K, Han X, Turner EE, Zeng H. A toolbox of Cre-dependent optogenetic transgenic mice for light-induced activation and silencing. *Nature neuroscience* 2012;15(5):793-802.
- [18] Mattis J, Tye KM, Ferenczi EA, Ramakrishnan C, O'Shea DJ, Prakash R, Gunaydin LA, Hyun M, Fenno LE, Gradinaru V, Yizhar O, Deisseroth K. Principles for applying optogenetic tools derived from direct comparative analysis of microbial opsins. *Nature methods* 2012;9(2):159-172.
- [19] Rein ML, Deussing JM. The optogenetic (r)evolution. *Molecular genetics and genomics : MGG* 2012;287(2):95-109.
- [20] Ringkamp M, Meyer RA. "Physiology of Nociceptors" in *The Senses: A Comprehensive Reference*. 2008;5:97-114.
- [21] Taylor AM, Peleshok JC, Ribeiro-da-Silva A. Distribution of P2X(3)-immunoreactive fibers in hairy and glabrous skin of the rat. *J Comp Neurol* 2009;514(6):555-566.
- [22] Usoskin D, Furlan A, Islam S, Abdo H, Lonnerberg P, Lou D, Hjerling-Leffler J, Haeggstrom J, Kharchenko O, Kharchenko PV, Linnarsson S, Ernfors P. Unbiased classification of sensory neuron types by large-scale single-cell RNA sequencing. *Nature neuroscience* 2015;18(1):145-153.
- [23] Vrontou S, Wong AM, Rau KK, Koerber HR, Anderson DJ. Genetic identification of C fibres that detect massage-like stroking of hairy skin in vivo. *Nature* 2013;493(7434):669-673.
- [24] Wang H, Zylka MJ. Mrgprd-expressing polymodal nociceptive neurons innervate most known classes of substantia gelatinosa neurons. *The Journal of neuroscience : the official journal of the Society for Neuroscience* 2009;29(42):13202-13209.
- [25] Zylka MJ, Rice FL, Anderson DJ. Topographically distinct epidermal nociceptive circuits revealed by axonal tracers targeted to Mrgprd. *Neuron* 2005;45(1):17-25.

## Figure legends

### Figure 1. Distribution of ChR2 in the somatosensory pathways of *TRPV1-ChR2* mice

The red signal represents the direct fluorescence of ChR2-tdTomato and the green signal shows P2X3 immunostaining. ChR2-tdTomato and the non-peptidergic marker P2X3 were mutually exclusive. A) In the dorsal horn of the spinal cord, tdTomato labeled lamina I and outer lamina II, dorsal to the P2X3 labeling in inner lamina II, confirming the selective ChR2 expression in peptidergic afferents. B) In glabrous skin, tdTomato fluorescence was observed in free nerve endings, some penetrating the epidermis. Red arrows show tdTomato<sup>+</sup> fibers and green arrows identify cutaneous P2X3<sup>+</sup> fibers. The dashed line indicates the border between dermis and epidermis. C) In dorsal root ganglia, tdTomato fluorescence was mainly found in small diameter neurons with 100% of tdTomato<sup>+</sup> cells expressing CGRP and only  $4.11 \pm 2.03\%$  expressing P2X3, indicating that ChR2-tdTomato was almost exclusively targeted to peptidergic nociceptors. Red arrows show tdTomato<sup>+</sup> neurons.

### Figure 2. Distribution of ChR2 in the somatosensory pathways of *MrgD-ChR2* mice

The green signal represents the direct fluorescence of ChR2-EYFP and the red signal shows CGRP immunostaining. ChR2-EYFP and the peptidergic marker CGRP are almost mutually exclusive. A) In the dorsal horn of the spinal cord, EYFP labeled the inner part of lamina II, ventral to the layer of CGRP<sup>+</sup> terminals, supporting the selective ChR2 expression in non-peptidergic afferents. B) In glabrous skin, EYFP fluorescence was observed in free endings terminating more superficially in the epidermis than CGRP-expressing fibers. Green arrows

show EYFP<sup>+</sup> fibers and red arrows identify CGRP<sup>+</sup> fibers. The dashed line indicates the border between dermis and epidermis. C) In dorsal root ganglia of *MrgD-ChR2* mice, EYFP fluorescence was mainly found in small diameter neurons with 100% of EYFP<sup>+</sup> cells binding IB4 and only  $0.92 \pm 0.68\%$  expressing CGRP, indicating that ChR2-EYFP was specifically delivered to non-peptidergic IB4<sup>+</sup> nociceptors.

**Figure 3. Electrophysiological phenotypes of dissociated ChR2<sup>+</sup> DRG neurons from *TRPV1-ChR2* and *MrgD-ChR2* mice**

A, B) Blue light (473 nm) stimulation (1 s,  $0.25 \text{ mW/mm}^2$ ) resulted in significant inward photocurrents in DRG neurons isolated from both *TRPV1-ChR2* and *MrgD-ChR2* mice. A) All tdTomato<sup>+</sup> DRG neurons isolated from *TRPV1-ChR2* mice responded to the TRPV1 agonist capsaicin (5  $\mu\text{M}$ ), validating the specific expression of ChR2 channels in peptidergic nociceptors (11/11 neurons). B) All EYFP<sup>+</sup> neurons isolated from *MrgD-ChR2* mice responded to the selective P2X3 agonist,  $\alpha,\beta$ -meATP (10  $\mu\text{M}$ ), indicating the specific expression of ChR2 channels in non-peptidergic nociceptors (8/8 neurons). Under current clamp, blue light pulses (1 Hz, 10 ms) reliably generated action potentials in ChR2<sup>+</sup> neurons from either *TRPV1-ChR2* or *MrgD-ChR2* mice. C) TRPV1<sup>+</sup> neurons always responded to capsaicin application and a proportion of them also responded to  $\alpha,\beta$ -mATP (6/11 neurons). Conversely, MrgD<sup>+</sup> neurons always responded to  $\alpha,\beta$ -mATP and some of them also responded to capsaicin (3/8 neurons). In response to  $\alpha,\beta$ -mATP, MrgD<sup>+</sup> cells showed a homomeric P2X3 current whereas heteromeric P2X2+3 currents were recorded in TRPV1<sup>+</sup> neurons.  $V_h = -60 \text{ mV}$  in voltage clamp and the mean resting membrane potential was  $-58.75 \pm 3.81 \text{ mV}$  in current clamp configuration ( $n = 8-11$  cells/genotype).

#### **Figure 4. Acute optically-evoked behaviors in *TRPV1-ChR2* mice**

Acute blue light stimulation (473 nm, 20 sec, X Hz) of the plantar surface of the hind paws of *TRPV1-ChR2* mice with increasing intensity and pulse frequency. This transgenic line displayed intensity-dependent stereotypical nocifensive behaviors such as paw withdrawal (A, B), lifting (C) and licking (D). The percentage of trials featuring each behavior is reported. Number of paw withdrawals was also calculated when such behavior occurred. Symbols represent mean  $\pm$  SEM ( $n = 9$  mice).

#### **Figure 5. Acute optically-evoked behaviors in *MrgD-ChR2* mice**

Acute blue light stimulation (473 nm, 20 sec, 2 Hz) of the plantar surface of the hind paws of *MrgD-ChR2* mice displayed distinct nocifensive behaviors such as paw withdrawal (A,B), lifting (C) and licking (D) in an intensity- and frequency-independent manner. The percentage of trials featuring each behavior is reported, as well as the number of paw withdrawals per trial when such behavior occurred. Symbols represent mean  $\pm$  SEM ( $n = 6$  mice).

#### **Figure 6. Distinct evoked behavioral responses between *TRPV1-ChR2* and *MrgD-ChR2* mice**

*TRPV1-ChR2* and *MrgD-ChR2* mice exhibited distinct stereotypical responses to acute transdermal blue light stimulation of the hind paw, especially regarding the time spent licking or lifting. A) *TRPV1-ChR2* mice showed a characteristic behavior in which they kept licking their paw for several seconds, whereas *MrgD-ChR2* mice never licked for a prolonged time, even at the highest light intensity and frequency. The time spent licking the paw under light stimulation at maximum intensity is depicted on the graph on the right. B) *MrgD-ChR2* mice spent

significantly more time lifting than *TRPV1-ChR2* mice under acute blue light stimulation, regardless of the light pulse frequency. The time spent lifting the paw under light stimulation at maximum intensity is depicted on the graph on the right. Symbols represent mean  $\pm$  SEM ( $n = 6-9$  mice). \*\*  $<0.01$  and \*\*\*  $<0.001$  using two-way ANOVA followed by Bonferroni post hoc test.

**Figure 7. Aversion to optogenetic stimulation more pronounced in *TRPV1-ChR2* mice than in *MrgD-ChR2* mice**

A) Using a conditioned place avoidance/preference paradigm, we assessed differential motivational effects of the activation of TRPV1<sup>+</sup> or MrgD<sup>+</sup> primary afferents by measuring the time spent in blue light- or yellow light-paired compartment during a 5 min session. B) Using an unbiased CPA paradigm, we did not observe any innate preference to either compartment before the conditioning session. C) Yellow light stimulation (parameters) did not induce place preference when compared to absence of light in *MrgD-ChR2* mice ( $n = 6$  mice). D) In *TRPV1-ChR2* mice, transdermal blue light stimulation (parameters) caused a strong aversion to the blue light-paired compartment. No place avoidance was displayed by *MrgD-ChR2* mice using the same conditioning parameters. ( $n = 8-12$  mice/group). Symbols represent mean  $\pm$  SEM. \*  $< 0.05$  using a Student's *t*-test.

Figure 1

**A** *TRPV1-ChR2*

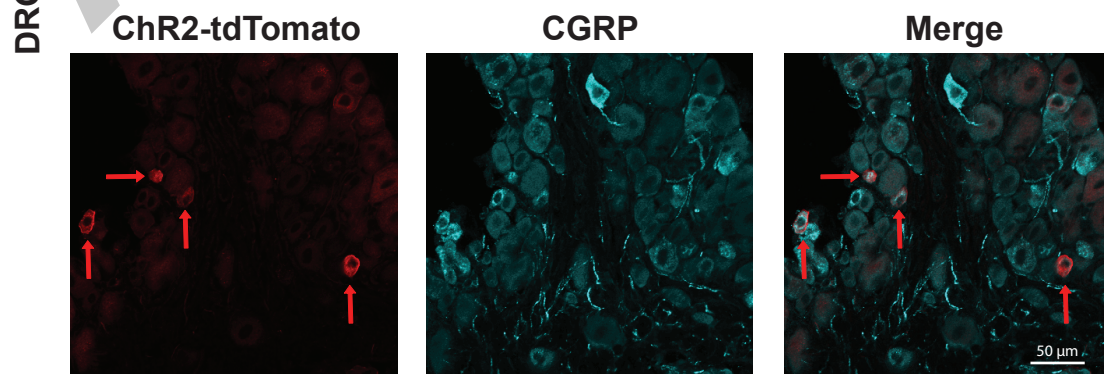
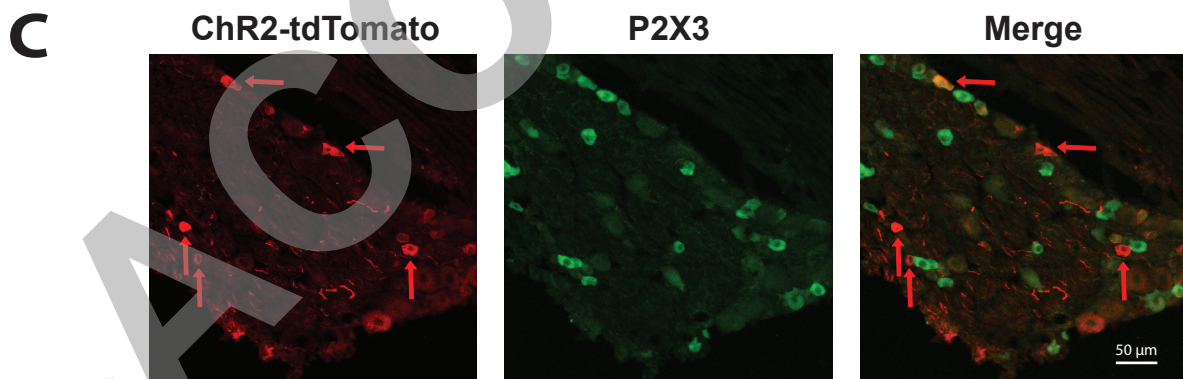
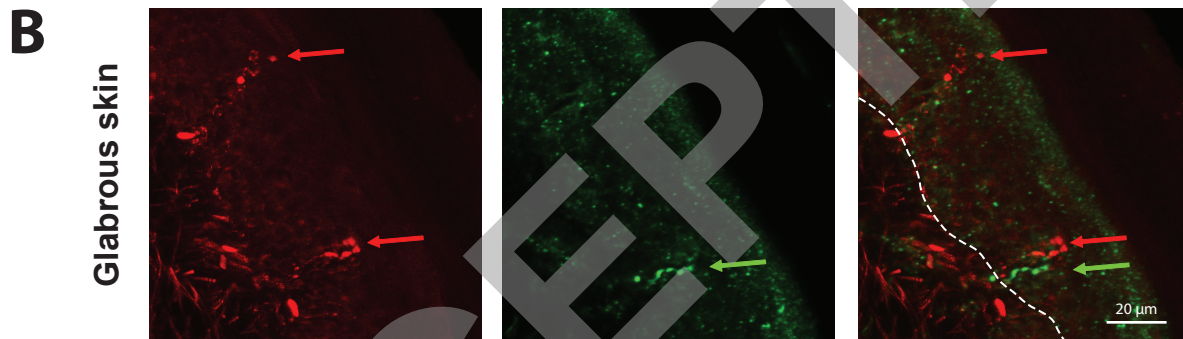
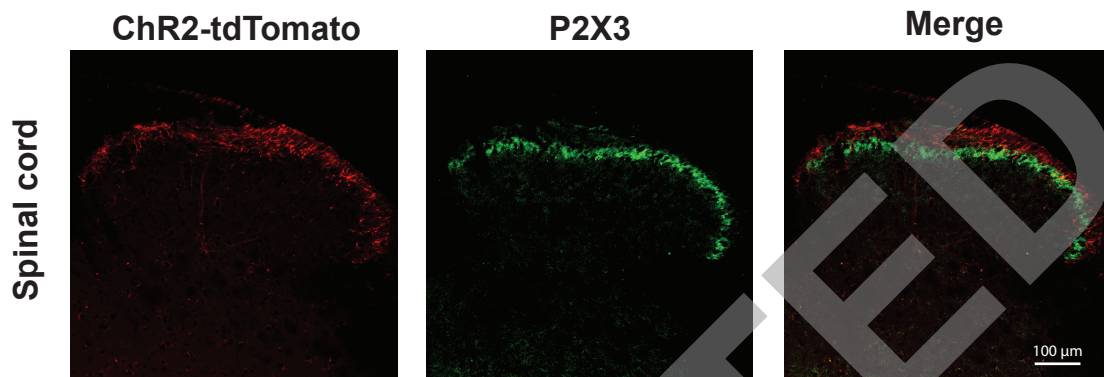
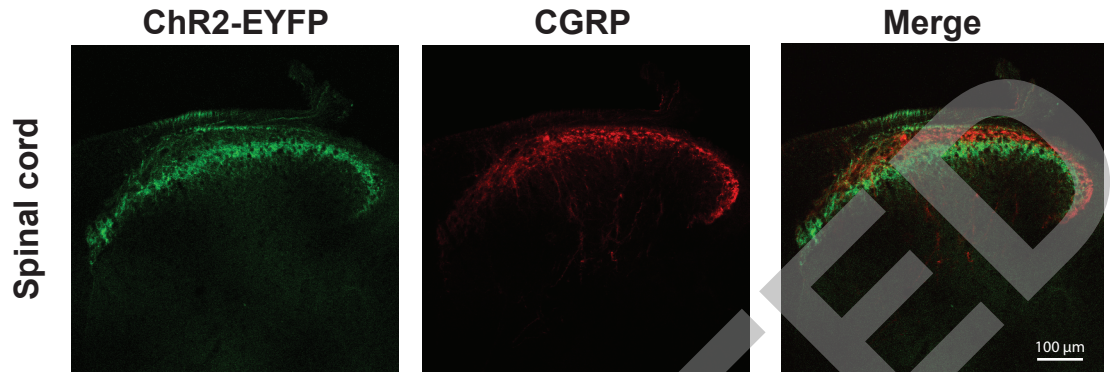
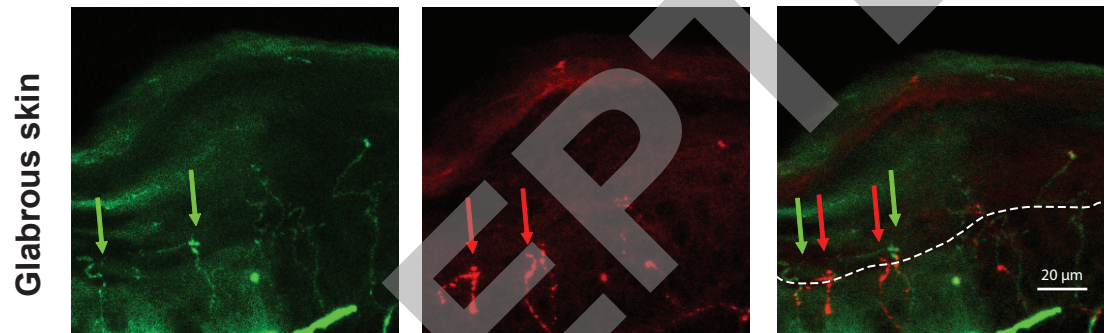


Figure 2

**A** *MrgD-ChR2*



**B**



**C**

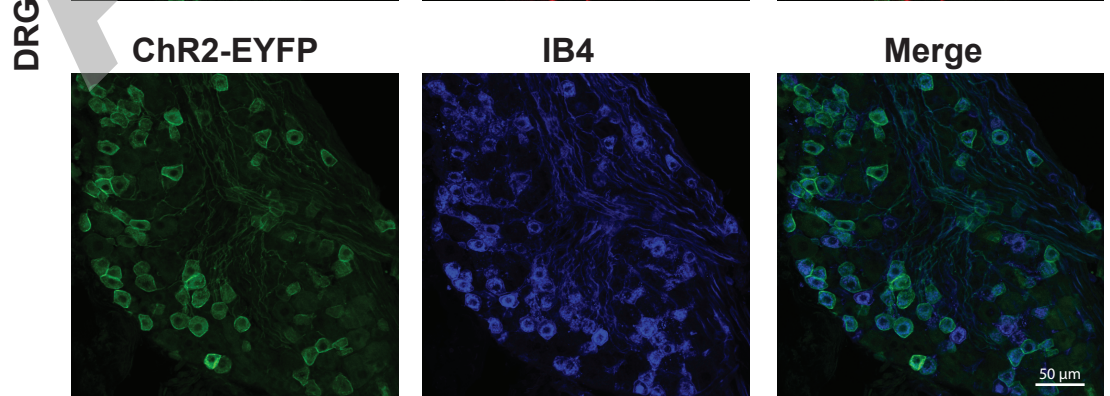
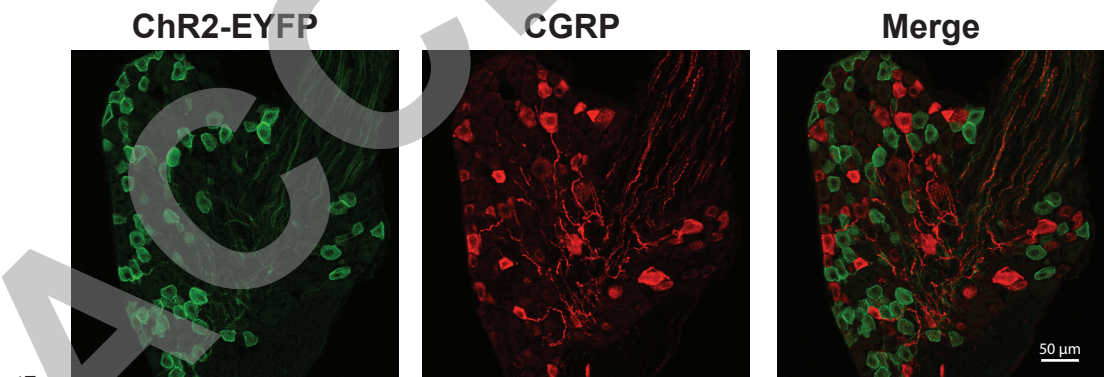
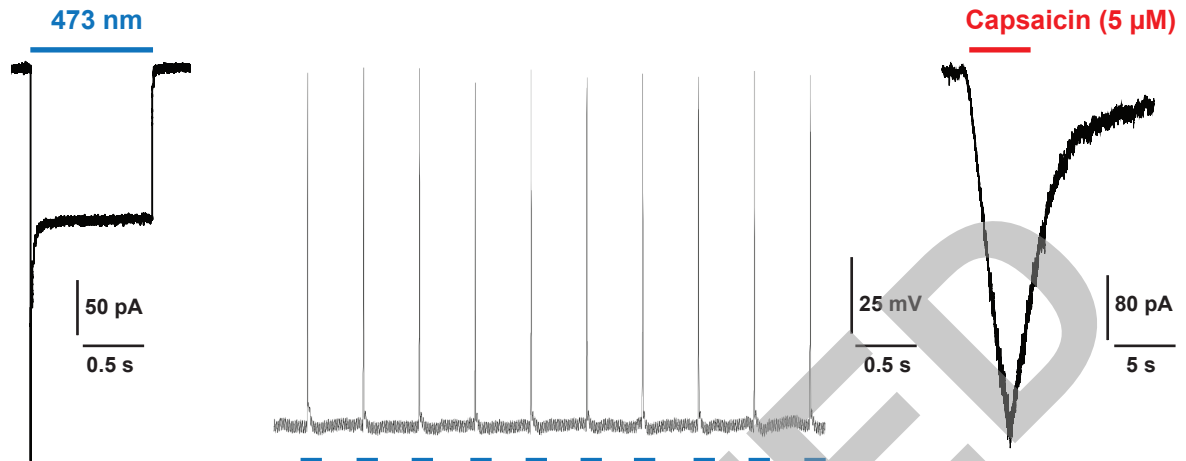


Figure 3

**A** tdTomato<sup>+</sup> DRG neurons from *TRPV1-ChR2* mice



**B** EYFP<sup>+</sup> DRG neurons from *MrgD-ChR2* mice



**C**

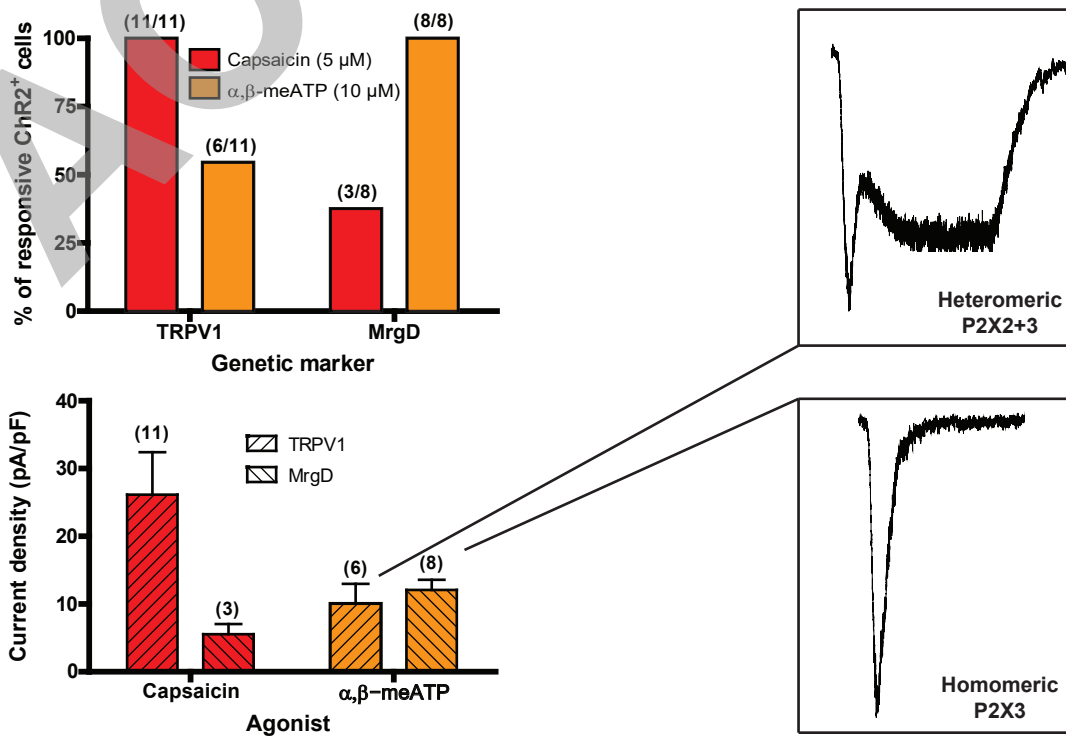


Figure 4

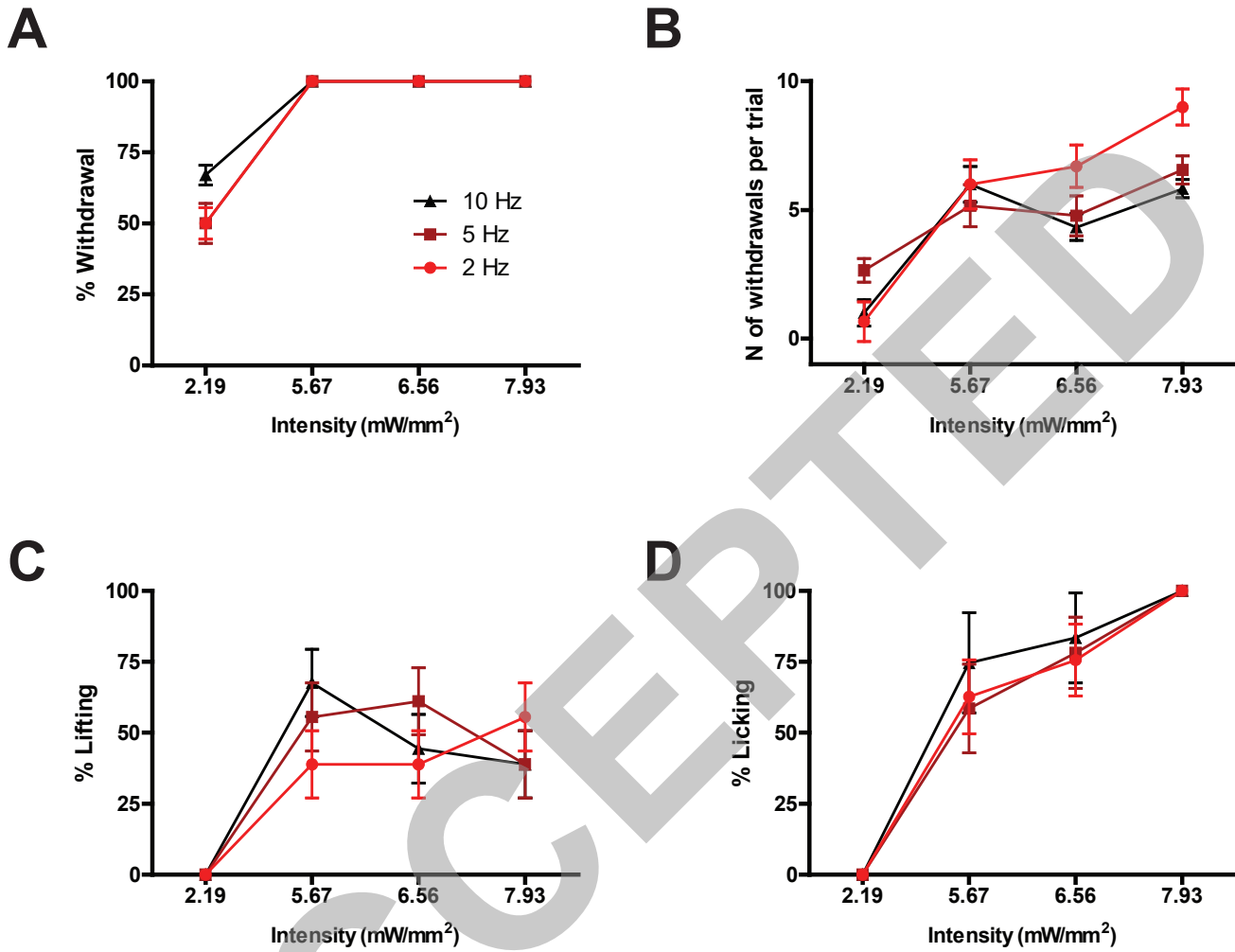


Figure 5

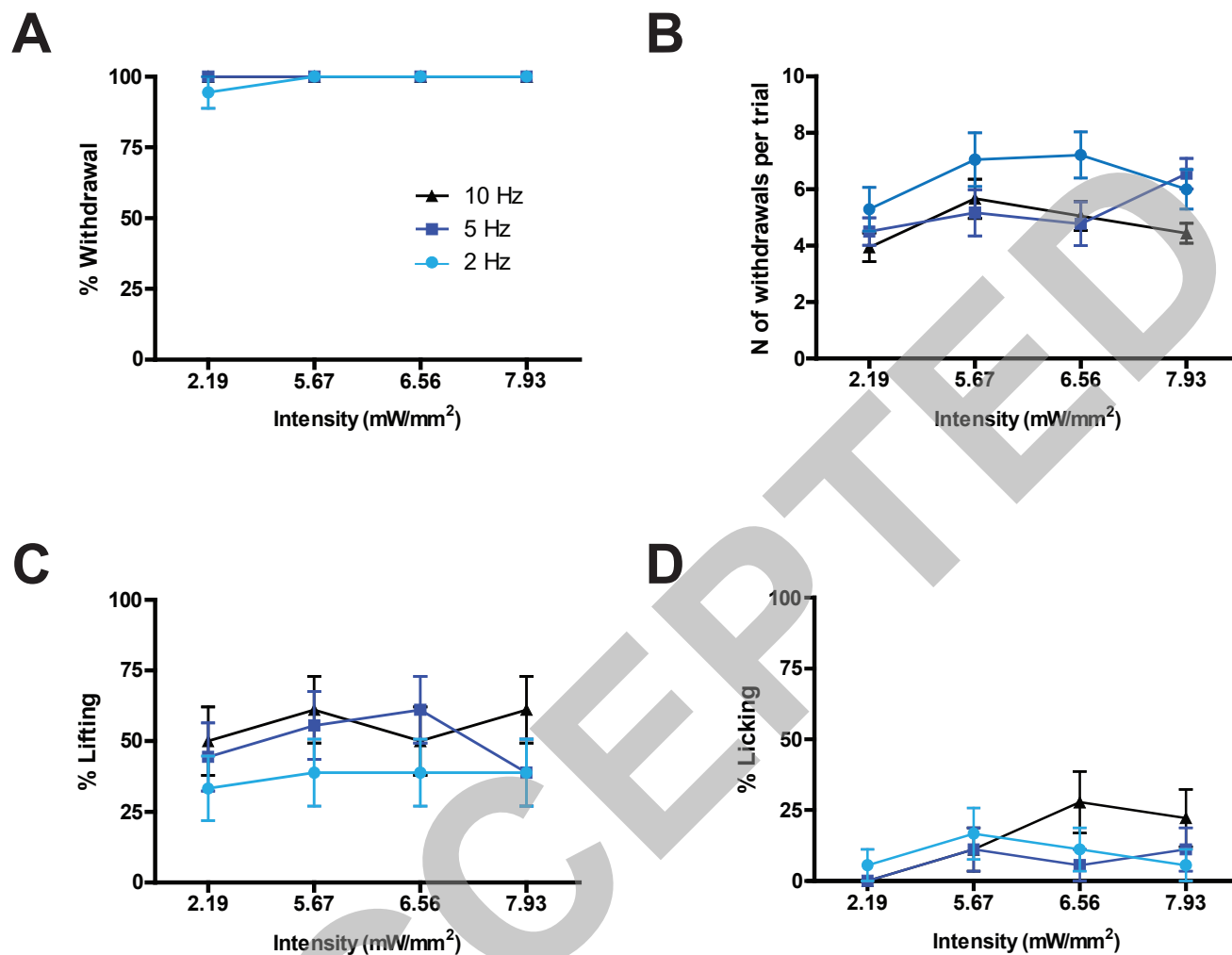


Figure 6

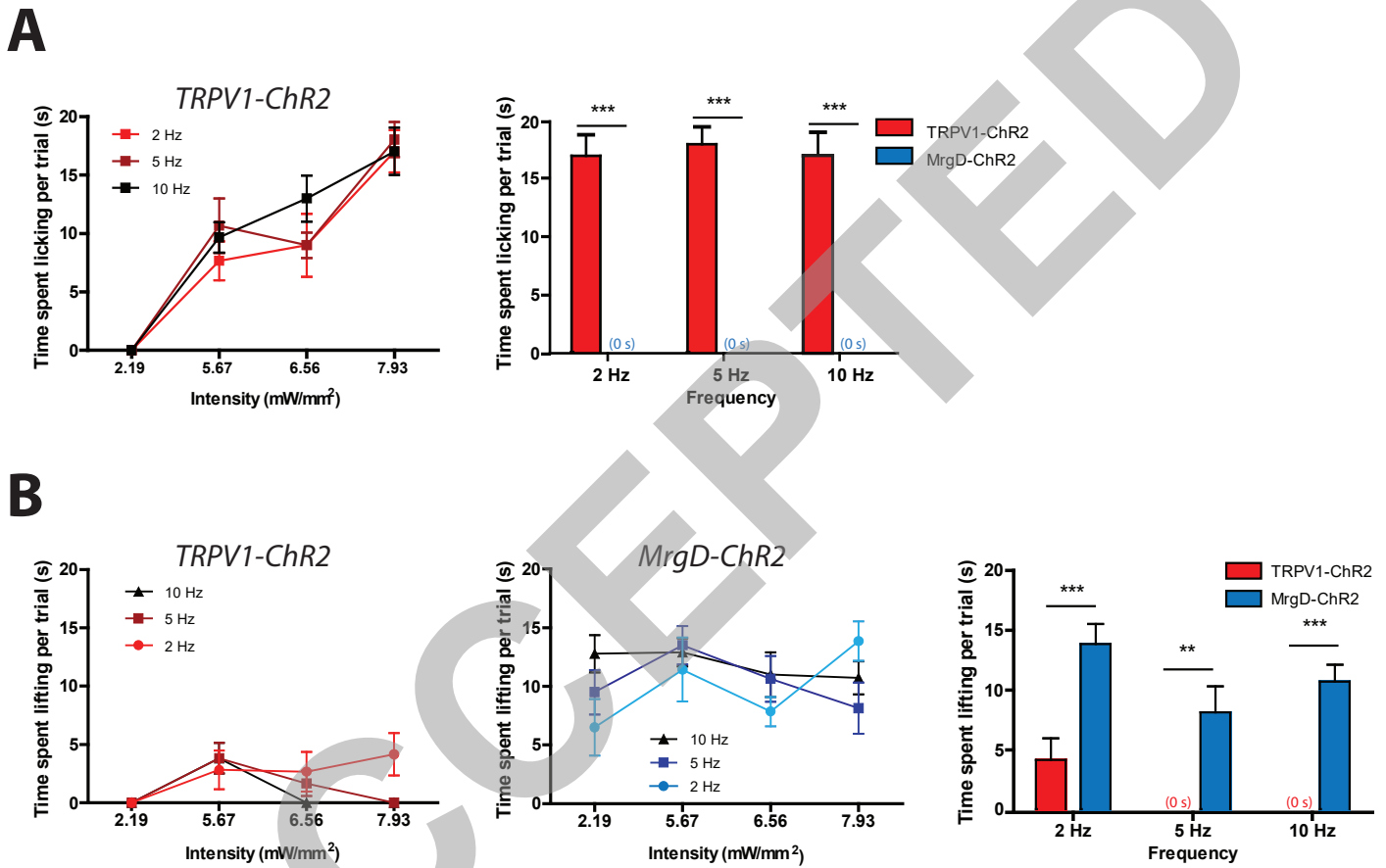


Figure 7

